Cure History Dependent Viscoelastic Modeling of Adhesively Bonded Joints using MAT_277 in LS-DYNA®

Akshat Agha*[1], Fadi Abu-Farha[1], Rakan Alturk[1], Tim Welters[2], Georges Romanos[2]
[1]*Clemson University - International Center for Automotive Research, Greenville, SC, USA*
[2]*Henkel Corporation, Düsseldorf, Germany*

Abstract

The effects of Coefficient of Thermal Expansion (CTE) mismatch in multi-material adhesive joints, induced during the manufacturing process, are expected to hinder the peak performance of the adhesive in the service life of the vehicle. With a goal to estimate these effects, this paper attempts to model the curing phenomenon of an adhesive and predict its mechanical properties using MAT_277 material model available in LS-DYNA, which serves as a good starting point towards modeling the cure history dependent viscoelastic behavior of adhesives. The adhesive is used to join two substrates of dissimilar metals and tested to capture the relative displacement of substrates. The experiments are performed on a specialized setup, which is built to perform experiments on lap shear joints. The curing kinetics model is calibrated using the results obtained by advanced experimental techniques like Differential Scanning Calorimetry (DSC); the mechanical properties are modeled by Generalized Maxwell model using Dynamic Mechanical Analysis (DMA) results. The fitted parameters are fed into MAT_277 to perform simulations of the lap shear joints tests. Finally, the calibrated model is validated by comparing the relative displacement in the steel-aluminum lap shear joint on a full curing cycle, similar to automotive paint baking oven, to experimentally obtained measurements using digital image correlation (DIC). The results of this work provide insights that will help in predicting the adhesive behavior over varying temperature-time histories during the manufacturing and in the service life of the vehicle.

Introduction

Automotive OEMs are competing in a race towards producing the most fuel-efficient cars in order to achieve the aggressive 2025 CAFÉ standards [1]. The ambitious fuel economy standards have set the attention of the industry to achieve more fuel efficiency by new means. In a study performed by Brooke and Evans, they showed that a 10% reduction in vehicle weight can result in 5-8% improvement in fuel economy [2,3]. In an automotive body dominated by different grades of steels, significant weight reduction is possible by material substitution. However, the most suitable advanced lightweight materials like aluminum and fiber reinforced plastics come at an increased price. To strike a balance between the weight reduction benefits and the vehicle cost, multi-material body parts serve as a viable solution.

The multi-material Body in White (BIW) design brings up the issue of multi-material joining where most of the joining techniques fail to deliver. Adhesives serve as a viable method for joining dissimilar materials like fiber reinforced plastics and non-ferrous metals. But, the fact that a structural adhesive needs to be cured at an elevated temperature poses a critical problem pertaining to different coefficients of thermal expansion (CTE) of joined parts, the mismatch of which has significant implications on the integrity and response of the BIW to external loading (mainly thermal). One of the main challenges when joining dissimilar materials is the assessment of the level and magnitude of residual stresses developing in the adhesive joint during the manufacturing process in case of hot-curing systems due to CTE mismatch of the different substrates.

By means of Finite Element Analysis (FEA), it is possible to predict the nature and magnitude of residual stresses in the adhesive bondline, which is otherwise impossible to measure by any reliable experimental technique [4,5,6]. FE models in combination with the experimental information of the curing kinetics, temperature and conversion dependent material properties of the adhesive can be used to assess the residual stress state and model the effects of CTE mismatch in the multi-material joint. The development of a suitable

modeling strategy is a challenge due to the complexity of the problem and the lack of readily available FEA implementations.
This paper serves to bridge that gap and provide insights that will help in modeling the adhesive behavior which can be scaled to the full vehicle level in a paint bake cycle during manufacturing or in environmental cycles during the service life.

Theory

The paint baking process of the BIW, which is also used for heat curing the adhesive, lasts approximately 30 minutes. As the body passes through the paint baking oven, the temperature of the body rises sharply to the range of 160-180°C and stays at that level for around 20 minutes before slowly cooling down to room temperature as shown in Figure 1 [7]. The paint baking cycle can hence be divided into (i) heating phase, when the body temperature rises, substrates expand freely and the adhesive slowly starts to cure, (ii) isothermal phase, when the adhesive cures hardens to a viscoelastic solid, while the substrates are in an expanded state (iii) cooling phase, when the temperature starts cooling and the adhesive picks up stresses due to the contraction of the adherends.

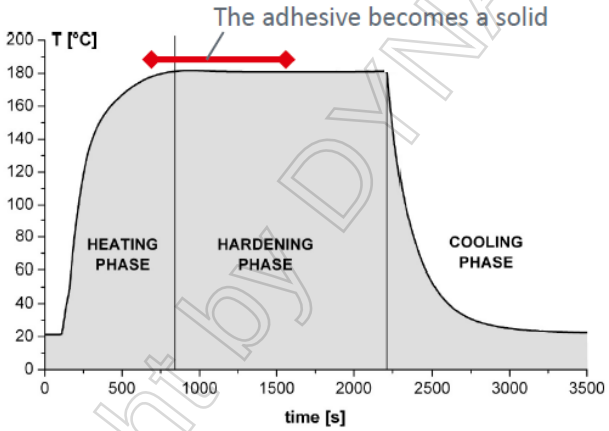

Figure 1. A generalized automotive paint bake cycle

Adhesives are known to show viscoplastic behavior. The viscoplastic properties of the adhesive depend on the level of cure attained during the manufacturing process. Therefore, it is necessary to determine the degree of cure in order to accurately predict the mechanical properties of the adhesive. Here, the study was restricted to the viscoelastic regime for simplicity.
In this approach, the material model is made of two components: (i) Curing Kinetics Model, which calculates the degree of cure depending on the temperature-time history; (ii) Mechanical Model, which takes input from the curing kinetics model and estimates the time-dependent viscoelastic behavior of the adhesive.
It is shown in several studies that the hot-cure adhesives exhibit chemical shrinkage while being cured. But, the stresses generated by shrinkage are relatively small for the adhesives and specimen geometries used here and researchers found that their values are not as significant for automotive applications as those generated by other phenomenon, such as CTE mismatch of substrates [7]. The measurement of shrinkage properties entails several tests on the Thermo-mechanical analyzer (TMA) [9], which has been skipped from the scope of this study in order to reduce model complexity but for sure is easily possible.

Methodology

Adhesive Material Model

The adhesive model implementation was done using *MAT_ADHESIVE_CURING_VISCOELASTIC (*MAT_277) in LS-DYNA which is capable of modeling the adhesive materials during chemical curing. The main advantage of using this material model is that the viscoelastic properties do not only depend on the temperature but also on an internal state variable which is the degree of cure (α) of the adhesive. The curing kinetics model is based on the temperature and the curing rate dependent Kamal model [10], which is given by:

$$\frac{d\alpha}{dt} = \left(k_1 \exp\left(\frac{-C_1}{RT}\right) + k_2 \exp\left(\frac{-C_2}{RT}\right)\alpha^m\right)(1-\alpha)^n$$

Where the rate of cure is a function of temperature T, and the degree of cure α. k_1 is the zero conversion rate value, k_2 is the auto-catalytic rate constant, C_1 and C_2 are representations of activation energy, m is the auto-catalytic exponent, n is the exponent for n^{th} order reaction model and R is the universal gas constant.

The relaxation functions of the viscoelastic Maxwell model are represented in this material formulation by up to 16 terms of the Prony series expansion given by the following equation [8,17]:

$$G(t,\alpha) = G_0(\alpha)\left(1 - \sum_i \frac{G_{i,\,\alpha=1.0}}{G_{0,\,\alpha=1.0}}(1 - e^{-\beta_i t})\right)$$

Where, $G_0(\alpha)$ is the instantaneous shear modulus as a function of degree of cure. While the 16 terms of the Prony series expansion are based on the shear modulus value at a full cure level. G_i is the shear relaxation modulus for the i^{th} term for fully cured material and β_i is the shear decay constant for the i^{th} term for fully cured material.

The adhesive mechanical properties at different temperatures are estimated using the WLF (Williams, Landel and Ferry) function [11] coded in the material card. This function makes use of the time-temperature superposition principle applicable to viscoelastic materials. The properties of viscoelastic materials recorded at one temperature can be superimposed upon data obtained at a different temperature simply by shifting one of the curves along frequency axis using a shift factor, which is approximated by WLF shift function. The shift factor is given by the following equation:

$$\Phi(T) = \exp\left(-A\frac{T - T_{REF}}{B + T - T_{REF}}\right)$$

Here, T_{REF} is the reference temperature at which properties are known, T is the current temperature, while A and B are curve fitting parameters.

Experiments for Model Calibration

The adhesive selected for the study was an epoxy-based automotive grade structural adhesive Teroson EP 5089 provided by Henkel Corporation. In order to describe the material behavior during the process as a function of the curing state of the adhesive, the curing kinetics model was calibrated by finding the parameters discussed above. A typical value of the conversion level α can be determined from the Differential Scanning Calorimetry (DSC) measurements. Several studies have been conducted in the past to determine the curing kinetics of epoxies using DSC data [4,12,13]. The heat flow through the adhesive sample was measured at different constant heating rates (0.5, 1, 2, 5, 10 and 20°C/min). A sample difference signal normalized with the adhesive weight for 1, 2 and 5°C/min is shown in Figure 2.

The enthalpy results from DSC were found to be independent of the heating rate. The results were integrated and numerically transformed into a curve showing the degree of cure vs temperature. The results for heating rates of 1, 2 and 5°C/min are shown in Figure 3.

Using isoconversional methods for activation energy calculation as discussed in previous publications [13,14,15] and using several numerical techniques, the data was fit to the Kamal model and the required parameters were obtained with a good fit for isothermal and non-isothermal DSC results. The DSC measurements for 0.5, 1, 2 and 5°C/min were used for model calibration and the measurements at 10 and 20°C/min were used for experimental verification of the calibrated curing kinetics model. A comparison between the experimental curve and predicted data for the degree of cure vs. temperature is shown in Figure 4.

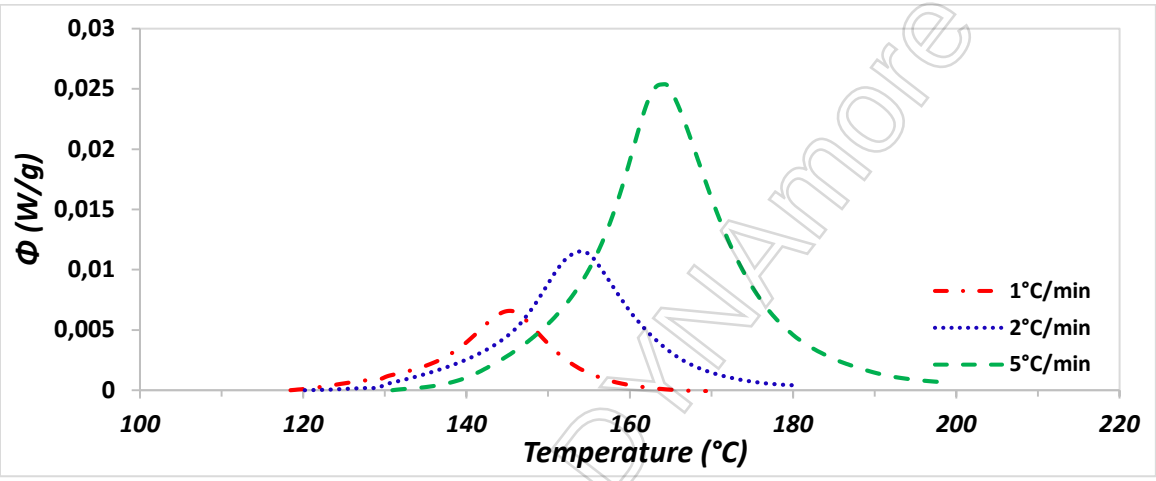

Figure 2. Sample DSC heat flow normalized with the specimen weight for different heating rates

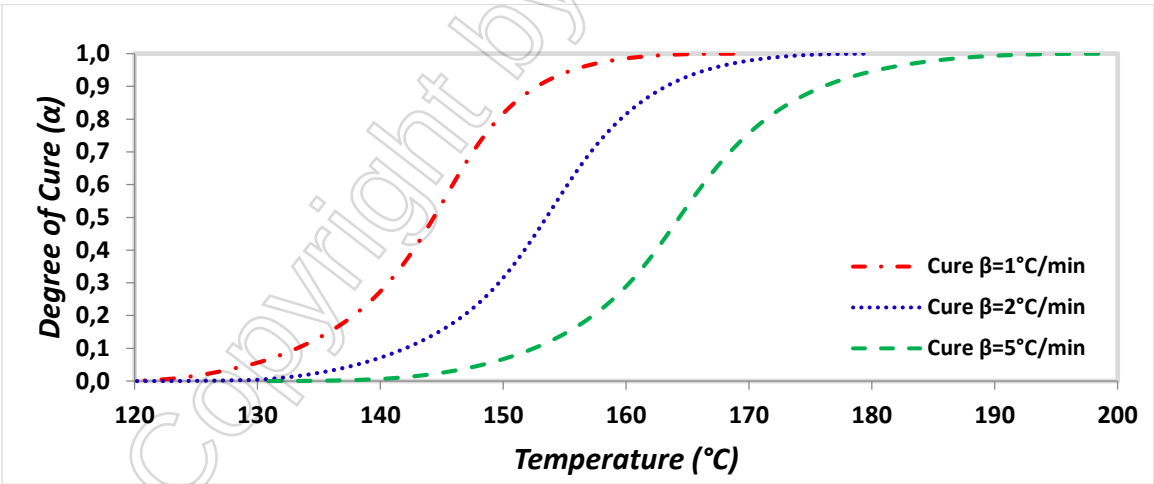

Figure 3. Degree of cure vs. Temperature obtained by numerical computations on DSC measurements.

The next task was the determination of parameters to model the mechanical properties as a function of cure and temperature. Dynamic Mechanical Analysis (DMA) measurements were done to find the elastic modulus values (later converted to shear modulus) as a function of decay time. The measurements were performed for a fully cured material, frequency sweep tests (storage and loss modulus) at temperatures ranging from -30°C to 150°C at a step of 5°C were performed (-30°C, -25°C, -20°C, ..., 150°C). The measured data was used to prepare a master curve of properties at 100°C (shown in Figure 5) by shifting the measurements towards left and right on the frequency axis to fall upon the chosen reference curve. The data sets from higher temperatures in the lower portion of the plot was shifted to the left (to lower frequencies) while those at lower temperatures were shifted

to the right (to higher frequencies). The shift factors were stored and later used to fit the WLF shift function [16]. A comparison of recorded shift factors with WLF function is shown in Figure 6.

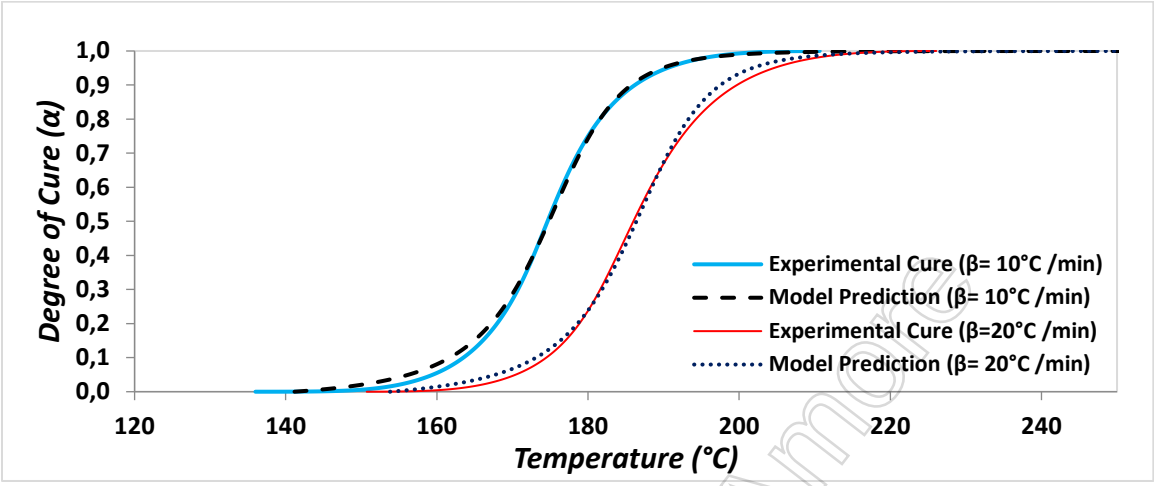

Figure 4. Comparison between predicted and measured data for degree of cure vs. temperature for heating rates of 10 and 20°C/min

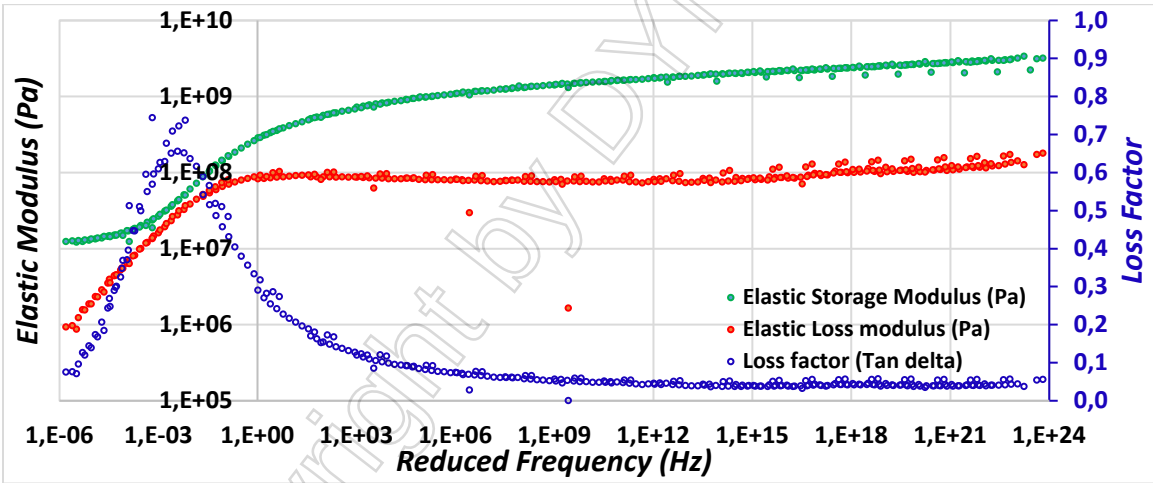

Figure 5. Master curves showing elastic storage, loss modulus and loss factor at 100°C

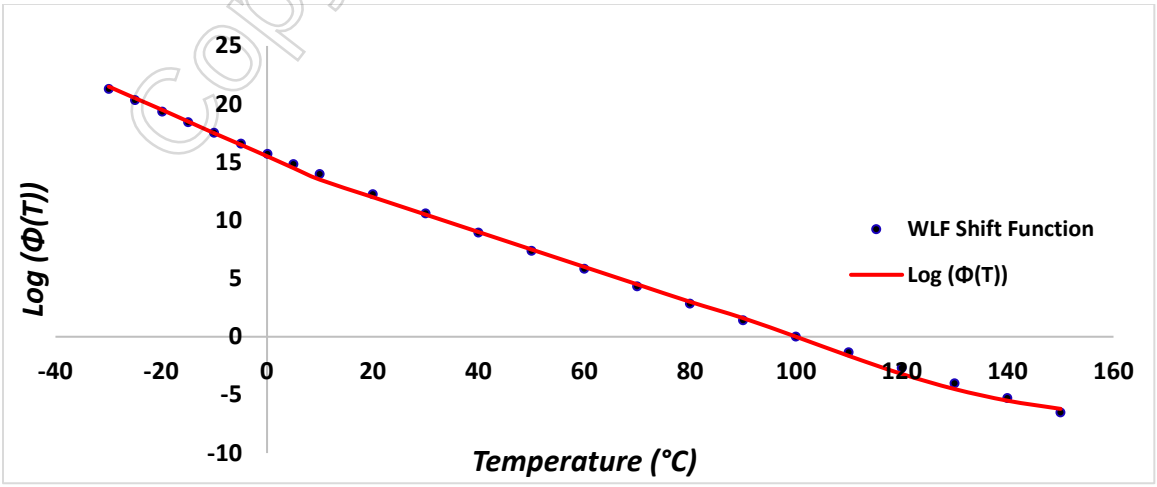

Figure 6. Comparison of Frequency Shift factors with fitted WLF Shift function

The developed master curve was then fit to 16 terms of Prony series expansion (allowed maximum in MAT_277) using numerical techniques and commercially available softwares [17]. A comparison of experimental shear properties and Prony series estimations is shown in Figure 7.

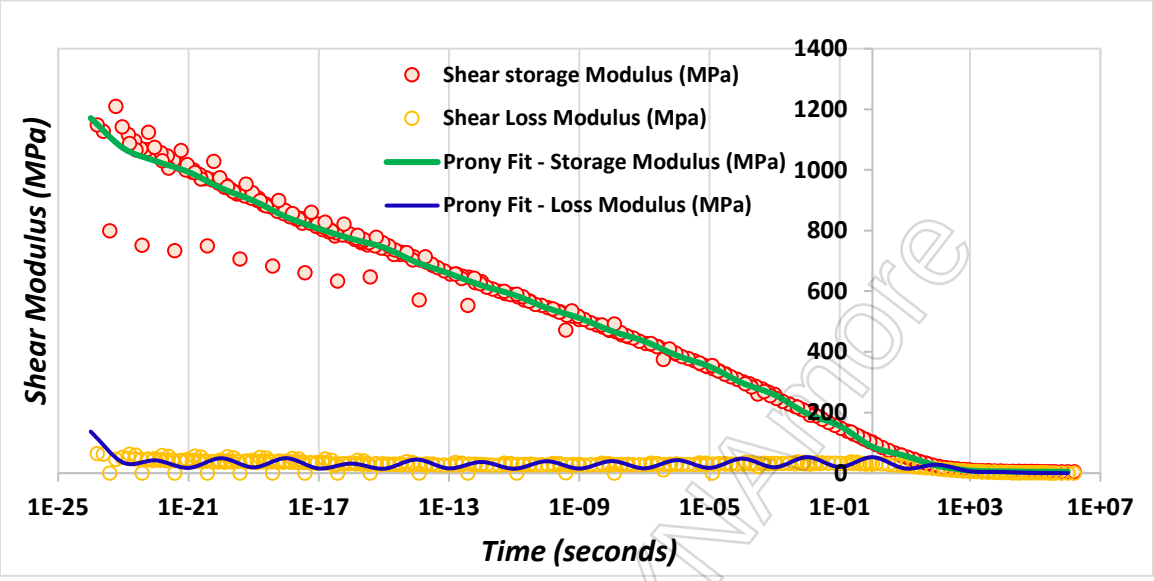

Figure 7. Comparison of measured experimental shear properties with Prony series estimation for storage and loss modulus

Experimental Validation

Experiments for Model Validation

A testing approach was developed to capture the thermal expansion effects in the adhesive joint while it is being cured. The experimental setup used for model validation was set on a universal load frame, similar to a tensile test setup. The setup was arranged to have the mounting grips and the specimen inside the furnace to simulate baking oven conditions. The furnace had a small glass window through which the specimen was monitored. Digital Image Correlation (DIC) cameras were set to capture the displacement in the substrates while the adhesive is curing. The grips used in the setup were made of a nickel-iron alloy with a very low coefficient of thermal expansion to minimize thermal expansion in the grip rods. The test setup is shown in Figure 8.

The tests were conducted on Aluminum-Steel joints using the structural adhesive Teroson EP 5089 provided by Henkel Corporation. The aluminum substrates were 1.22 mm thick pieces of AA6111-T4, while the steel substrates were 0.80 mm thick pieces of Mild steel (CR5). The size of the substrates was 100 mm x 20 mm. The measured adhesive bondline thickness was approximately 0.2 mm. The test samples were prepared by applying the uncured adhesive between two metal substrates to form a lap shear joint as shown in Figure 9. The samples were held together using a clip to avoid rotation in the sample in the uncured state. The samples were painted to form speckle pattern over the target region for optical strain measurements using DIC, and simultaneously the force exerted on the grips due to thermal expansion was recorded.

The tests were started at room temperature at t=0 and the furnace temperature was set to reach 180°C. The heating was stopped at t=40 mins and the furnace door was opened to allow the specimen to cool down to the room temperature. The temperature of the furnace was measured by the furnace thermocouple while a K – type thermocouple was attached to the back of the specimen to record the specimen temperature during the experiment. An example of the recorded specimen temperature profile along with analytically calculated degree of cure value is shown in Figure 10.

The DIC data was processed to calculate the relative displacement at two points 50 mm away on the two substrates as discussed in the next section.

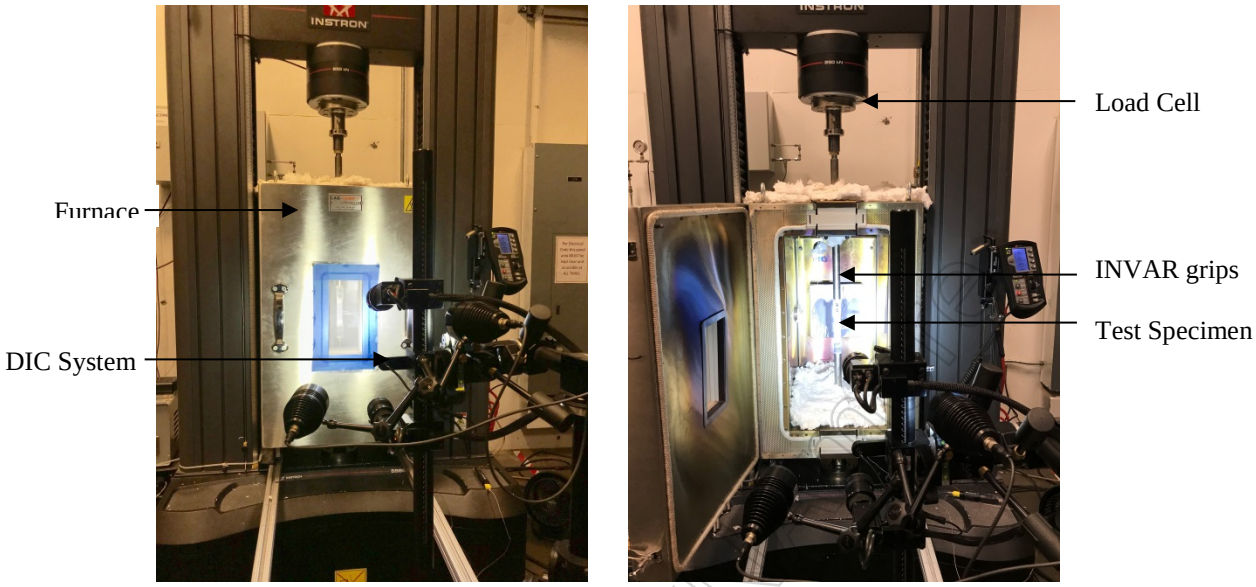

Figure 8. Test setup used for the experimental validation Heating (L), and cooling (R)

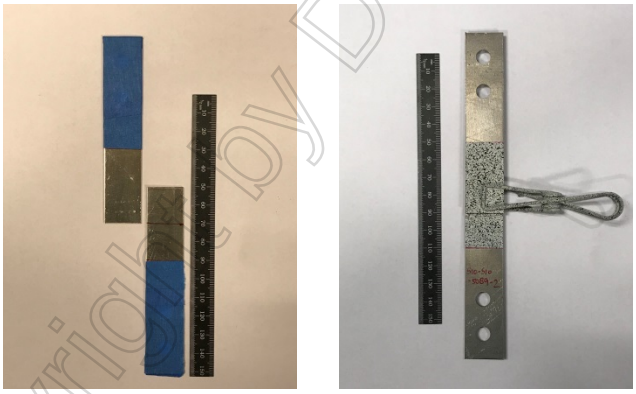

Figure 9. Unbonded substrates (L) and painted test specimen ready for testing (R)

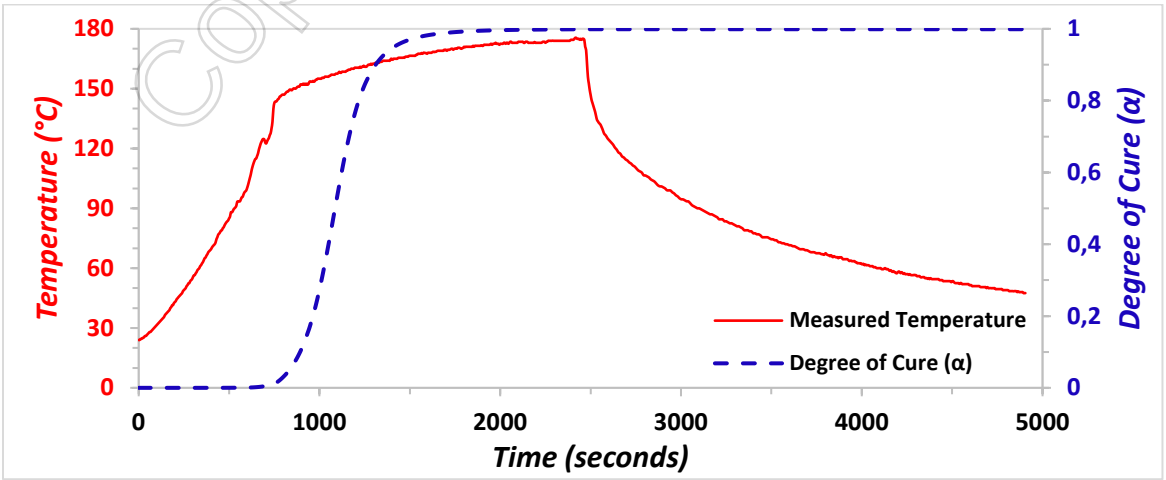

Figure 10. Experimentally measured specimen temperature vs. Degree of cure (α)

Finite Element Model

Specimen Geometry

The specimen geometry used for the FE model was based on the specimen used for experiments as shown in Figure 11. The substrates were 100 mm long and 20 mm wide. The overlap length was 20 mm, hence the adhesive joint dimensions were 20 mm x 20 mm. The adhesive bondline thickness was kept as 0.2 mm based on the experimentally recorded value.

The metal substrates were modeled using shell elements using the material model *MAT_ELASTIC_PLASTIC_THERMAL (*MAT_004). The thermal model used in the simulation was *MAT_THERMAL_ISOTROPIC_TD_LC (*MAT_T10). The adhesive layer between the two substrates was modeled as 3D solid elements using MAT_277. A layer of null shell elements *MAT_NULL (*MAT_009) was used between the shell and solid elements to model the contact layer. The contact definition *CONTACT_TIED_SURFACE_TO_SURFACE was used to model the contact boundary between the solid adhesive and the shell substrates.

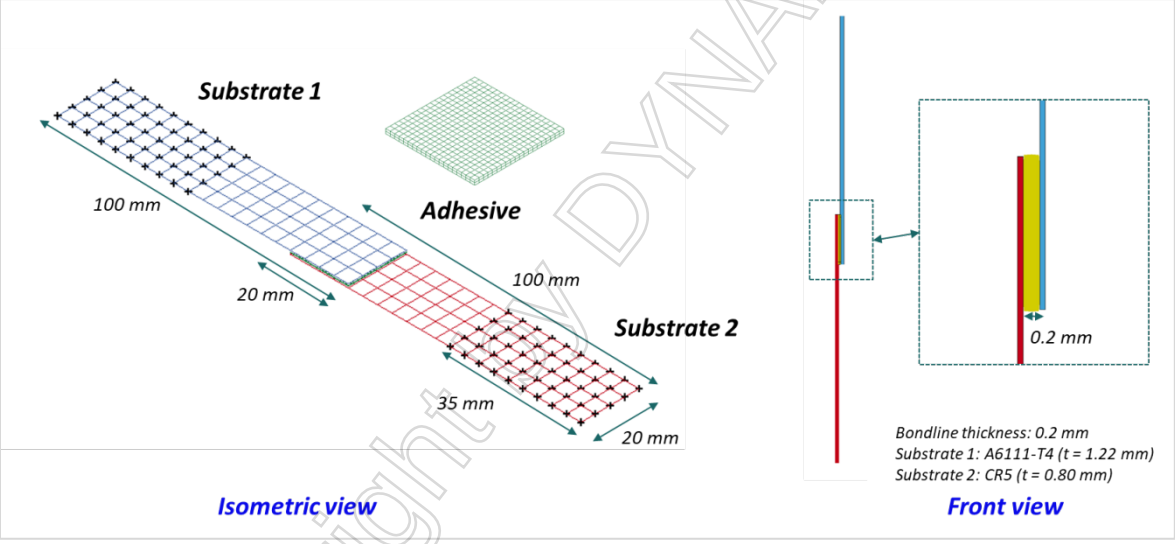

Figure 11. Specimen Geometry used for the experiments and the FE model

Boundary Conditions and Constraints

The specimen was constrained at the top and bottom up to a length of 35 mm from the ends, to make the free length exactly the same as the tested specimen; this is shown in Figure 11.

The temperature profile obtained from the furnace thermocouple and the thermocouple attached to the specimen surface was used to calculate the convective heat transfer coefficient, h, which is fed into the FE model. The *BOUNDARY_CONVECTION keyword in LS-DYNA was used to simulate the heat transmission to the specimen.

A cycle time of 5000 seconds is too long and computationally expensive with the typical time steps used for solid adhesive mesh. The calculation was time-scaled by 10000x and the termination time was set to 0.5 seconds to speed up the computation time.

Results

The relative displacement in the two substrates during the curing process and the final displacement was measured in the experiments by processing the DIC results. The comparison was made by creating a virtual

extensometer of 50 mm length across the joint, with one end on each substrate as shown in Figure 12. The change in the Y-direction and Z-direction were obtained using DIC measurements.

A comparison of experimentally obtained DIC result vs. LS-DYNA prediction of Y-displacement is shown in Figure 13. There was an experimentally measured residual displacement of 0.11 mm in the Y-direction, at the end of the temperature cycle. The predicted residual Y-displacement was 0.10 mm. As the temperature starts rising, the substrates begin to thermally expand and come close to each other due to the constraints from the

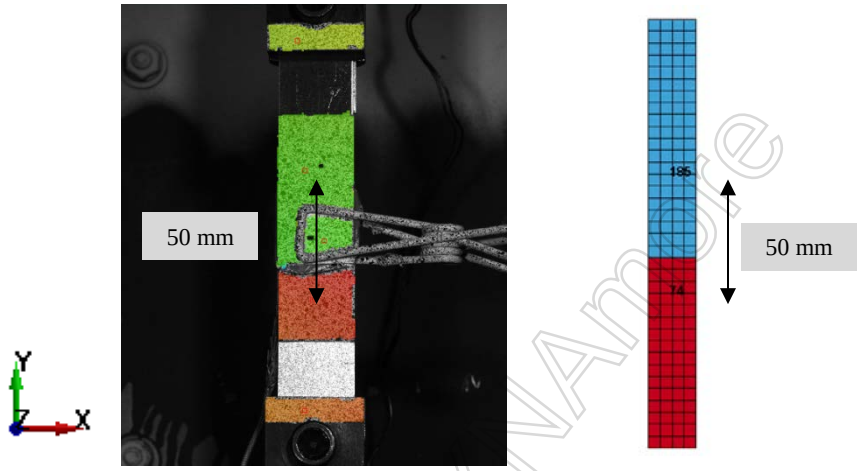

Figure 12. DIC processed image (L) and finite element model geometry (R) showing the two points 50mm apart

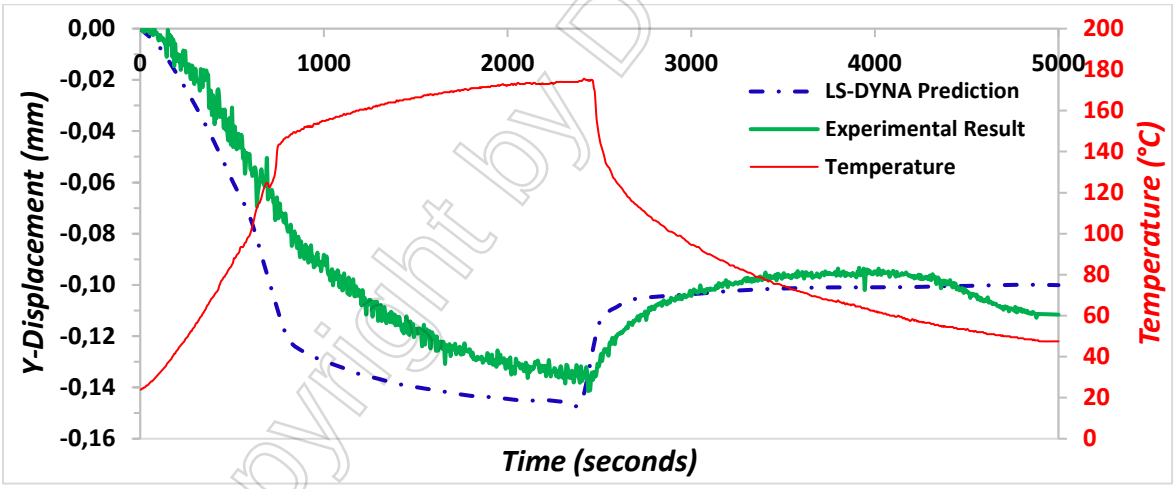

Figure 13. Experimental vs. Predicted displacement in Y-direction

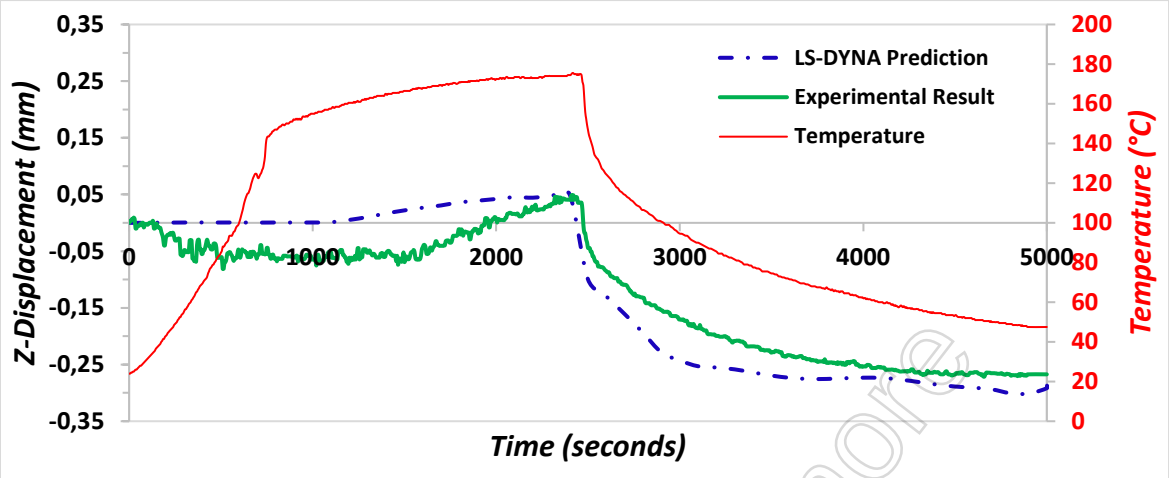

Figure 14. Experimental vs. Predicted displacement in Z-direction

grips. This is represented by a negative displacement in the beginning. The substrates move freely as the adhesive is in a viscoelastic liquid state and does not pose any restriction to the movement. During the isothermal condition, the adhesive cures and changes to a viscoelastic solid state. In the cooling phase, when the Adherends begin to contract, the fully cured adhesive poses restriction to the return movement of the adherends. This in turn puts shear stresses on the adhesive and results in a residual displacement in the joint.

A comparison of the displacement in the Z-direction is shown in Figure 14. A residual displacement of 0.27 mm was observed in the Z direction in the experiments. The LS-DYNA prediction of 0.29 mm was very close to the experimentally obtained result. The Z-displacement shows the bending in the substrates on joining. The distortion happens in the cooling phase when the adherends try to contract in the Y-direction against the adhesive force. The restriction causes the adherends to bend in the Z-direction.

The heat transfer coefficient, h was calculated based on the temperature measurements made on a single point on one substrate, while the temperature profile within the volume of the furnace may actually vary to a certain degree along the specimen. Considering this limitation, the predicted relative displacements are in an excellent correlation with the experimental recordings.

The predicted residual stress state in the adhesive is shown in Figure 15. The adhesive starts developing noticeable stresses as the gelification starts (at approximately α=0.6). The YZ-shear stress changes direction and starts developing rapidly as the specimen starts to cool and reaches a magnitude of 8 MPa at the end of the temperature cycle, while the effective Von-Mises stress in the adhesive element is of the order of 15 MPa. The adhesive picks up stresses more rapidly on cooling since the shear modulus of the adhesive is higher at lower temperatures.

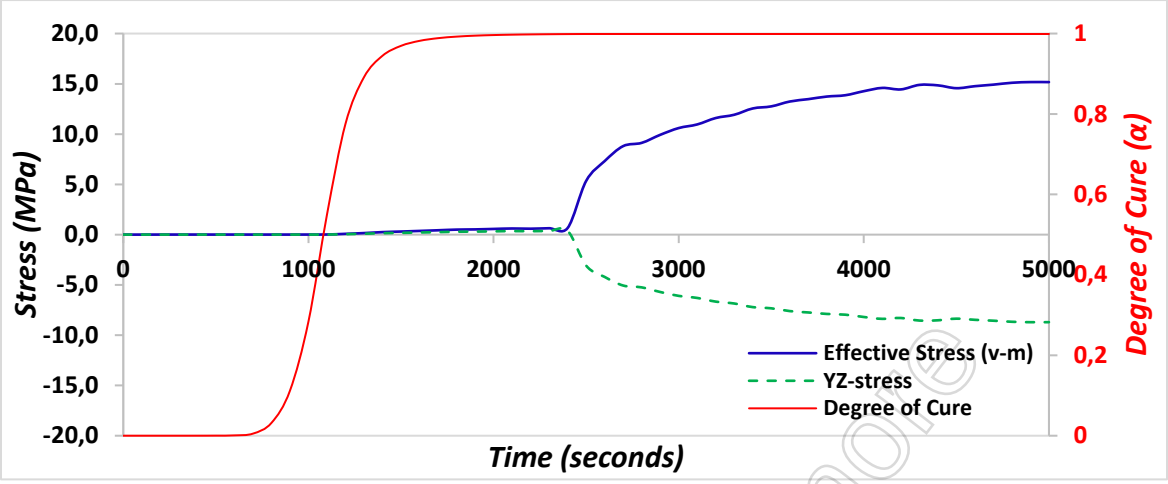

Figure 15. Predicted residual stresses in the adhesive vs. Degree of cure and time

Summary

In this work, MAT_277 in LS-DYNA was used to model the CTE mismatch effects in multi-material adhesive bonded joints. The experimental techniques to calibrate the curing kinetics model and the mechanical model were discussed. The calibrated model was tested on a lap shear joint for automotive paint bake cycle by the aid of digital image correlation (DIC). The developed model is capable of predicting the distortion effects of CTE mismatch on the joint to a satisfactory level. The predicted residual stresses in the adhesive of this magnitude prove that more attention is required in this area as the residual stress is nearly 30% of the ultimate shear strength of the lap-shear adhesive joint. For future work, there is a scope of improvement in the stress-strain formulation of the material card. Addition of a plastic component to the mechanical model is required for crash based simulation to capture the effect of curing on plastic behavior responsible for crash performance. Second, the shrinkage strain in the adhesive can also be taken into account for more accurate prediction of the CTE mismatch effects.

Acknowledgements

The authors would like to thank Henkel Corporation North America and Henkel Corporation Germany for sponsoring and providing valuable inputs to this study.

References

1. Bento, Antonio M., Kevin D. Roth, and Yiwei Wang. "The Impact of CAFE Standards on Innovation in the US Automobile Industry." In Agriculture and Applied Economics Association, 2015 AAEA & WAEA Joint Annual Meeting, pp. 26-28. 2015.
2. Wagner, Markus, A. Jahn, and B. Brenner. "Innovative joining technologies for multi-material lightweight car body structures." In Proceedings of the International Automotive Body Congress (IABC), Dear-born, pp. 29-30. 2014.
3. Brooke, L., Evans, H., "Lighten Up!", Automotive Engineering, 117, 2009, 16 - 22)
4. Dong, Sheng, Anthony Smith, and Allen Sheldon. "Modeling of Curing Adhesives between Jointed Steel and Aluminum Plates using MAT_277 in LS-DYNA.", 2017.
5. Jamie M. Kropka, Mark E. Stavig and Robert S. Chambers. "Role of Residual Stress on the Strength of Adhesive Joints." Sandia National Laboratories SAND2013-10717C (2013).
6. Marques, E. A. S., Lucas F. M. da Silva, M. D. Banea, and R. J. C. Carbas. "Adhesive Joints for Low- and High-Temperature Use: An Overview." The Journal of Adhesion 91, no. 7 (2014): 556-85. http://dx.doi.org/10.1080/00218464.2014.943395.
7. R.A. Dickie*, D.R. Bauer, S.M. Ward, D.A. Wagner. "Modeling Paint and Adhesive Cure in Automotive Applications." *Progress in Organic Coatings* 31 (1997) 209–216 (1997).
8. Drabousky, David Peter. "Prony Series Representation and Interconversion of Viscoelastic Material Functions of Equine Cortical Bone." Case Western Reserve University (August, 2009)
9. Daoqiang Lu, C.P. Wong*. "Effects of Shrinkage on Conductivity of Isotropic Conductive Adhesives." International Journal of Adhesion & Adhesives 20 (2000) no. 20 (2000): 189-93.
10. Kamal, Musa R. "Thermoset characterization for moldability analysis." Polymer Engineering and Science 14, no. 3 (1974): 231-39. doi:10.1002/pen.760140312.
11. Malcolm L. Williams, Robert F. Landel, and John D. Ferry. "The Temperature Dependence of Relaxation Mechanisms in Amorphous Polymers and Other Glass-Forming Liquids." Journal of the American Chemical Society 77 (14) (1955): 3701–07
12. Hardis, Ricky, Julie LP Jessop, Frank E. Peters, and Michael R. Kessler. "Cure kinetics characterization and monitoring of an epoxy resin using DSC, Raman spectroscopy, and DEA." Composites Part A: Applied Science and Manufacturing 49 (2013): 100-108.
13. Badrinarayanan, Prashanth, Yongshang Lu, Richard C. Larock, and Michael R. Kessler. "Cure Characterization of Soybean Oil-Styrene-Divinylbenzene Thermosetting Copolymers." Journal of Applied Polymer Science 113, no. 2 (2009): 1042-49. http://dx.doi.org/10.1002/app.29776.
14. Duemichen, E., M. Javdanitehran, M. Erdmann, V. Trappe, H. Sturm, U. Braun, and G. Ziegmann. "Analyzing the Network Formation and Curing Kinetics of Epoxy Resins by in Situ near-Infrared Measurements with Variable Heating Rates." Thermochimica Acta 616 (2015): 49-60. http://dx.doi.org/10.1016/j.tca.2015.08.008
15. Xiao-Wang Yang, SHao-Rong Lu, Yu-Mei Jiang, Bo Zhang and Jin-Hong Yu. "Preparation and Curing Kinetics Investigation of Diglycidyl Ether of Bisphenol a/Liquid Crystalline Epoxy Resin Blends." Iranian Polymer Journal 17 (4), 2008, 251-264 (April 2008)
16. Instruments, TA. "Thermal Analysis Application Brief." Thermal Analysis and Rheology TA-144
17. YAN Hongqing1, 2, ZHANG Xiaoning 2 and ZHANG Lijuan2. "Methods of Fitting the Prony Series of Viscoelastic Model of Asphalt Mixture Based on Dynamic Modulus." *ICTE 2011 © ASCE 2011* (2011).